Interactions of Substrates at the Surface of P450s Can Greatly Enhance Substrate Potency[†,‡]

Amita Hegde,[§] Donovan C. Haines,[||] Muralidhar Bondlela,[§] Baozhi Chen,[§] Nathaniel Schaffer,[§] Diana R. Tomchick,[§] Mischa Machius,[§] Hien Nguyen,[||] Puneet K. Chowdhary,[||] Larissa Stewart,[||] Claudia Lopez,[||] and Julian A. Peterson*[,§]

Department of Biochemistry, The University of Texas Southwestern Medical Center at Dallas, Dallas, Texas 75390-9038, and Department of Chemistry, The University of Texas at Dallas, Dallas, Texas 75083-0688

Received August 17, 2007; Revised Manuscript Received September 29, 2007

ABSTRACT: Cytochrome P450s are a superfamily of heme containing enzymes that use molecular oxygen and electrons from reduced nicotinamide cofactors to monooxygenate organic substrates. The fatty acid hydroxylase P450BM-3 has been particularly widely studied due to its stability, high activity, similarity to mammalian P450s, and presence of a cytochrome P450 reductase domain that allows the enzyme to directly receive electrons from NADPH without a requirement for additional redox proteins. We previously characterized the substrate *N*-palmitoylglycine, which found extensive use in studies of P450BM-3 due to its high affinity, high turnover number, and increased solubility as compared to fatty acid substrates. Here, we report that even higher affinity substrates can be designed by acylation of other amino acids, resulting in P450BM-3 substrates with dissociation constants below 100 nM. *N*-Palmitoyl-L-leucine and *N*-palmitoyl-l-methionine were found to have the highest affinity, with dissociation constants of less than 8 nM and turnover numbers similar to palmitic acid and *N*-palmitoylglycine. The interactions of the amino acid side chains with a hydrophobic pocket near R47, as revealed by our crystal structure determination of *N*-palmitoyl-l-methionine bound to the heme domain of P450BM-3, appears to be responsible for increasing the affinity of substrates. The side chain of R47, previously shown to be important in interactions with negatively charged substrates, does not interact strongly with *N*-palmitoyl-l-methionine and is found positioned at the enzyme−solvent interface. These are the tightest binding substrates for P450BM-3 reported to date, and the affinity likely approaches the maximum attainable affinity for the binding of substrates of this size to P450BM-3.

Cytochrome P450BM-3 (P450BM-3, CYP102A1) is a fatty acid monooxygenase that was isolated from *Bacillus megaterium* by Fulco and co-workers (*1*, *2*) and is a fusion protein between a cytochrome P450 and an FAD[1]/FMN containing NADPH-P450 reductase (*3*, *4*). Similar fusion proteins have now been found in the genomes of at least 16 microorganisms (NCBI). The exact function of P450BM-3 in *B. megaterium* is unknown, but it has been shown to metabolize a range of saturated and unsaturated fatty acids with chain lengths from 12 to 22 carbon atoms (*5*). P450BM-3 was initially shown to be induced in *B. megaterium* by phenobarbital or acyl ureas, but clearly, these compounds are not the physiological inducers or even substrates of P450BM-3 (*6*, *7*). More recently, P450BM-3 has been shown to be induced by nonsteroidal anti-inflammatory drugs (*8*) and branched chain fatty acids such as phytanic acid (*9*). Wolf's group also showed that polyunsaturated fatty acids are toxic to *B. megaterium* and that genetic or chemical inactivation of P450BM-3 increases the toxicity of the fatty acids (*10*). These data led to the presumption that this P450 is present to detoxify polyunsaturated fatty acids. In vitro, the fatty acid with the highest turnover number, at up to 6000 min^{-1}, is arachidonic acid, which is converted to 20% 14(*S*),15(*R*)-EET and 80% 18-(*R*)-OH-AA (*11*). Another frequently studied substrate is palmitic acid, with a turnover number of 2000 min^{-1} and a product profile of 25% 15(*R*)-OH-PA, 50% 14(*R*)-OH-PA, and 25% 13(*R*)-OH-PA (*5*, *12*). The conserved structural fold and catalytic mechanism among P450s (*13*), as well as the ease of purification and handling of P450BM-3, has made this enzyme an excellent prototype for eukaryotic P450s and specifically for fatty acid metabolizing P450s. The experiments described here were undertaken to better understand the mechanism of substrate recognition and binding of fatty acid substrates in P450s.

[†] This work was supported in part by NIH Grants GM43479 and GM50858 (J.A.P.) and the Welch Foundation (AT-1600, D.C.H.).

[‡] Coordinates and structure factors have been deposited in the Protein Data Bank under Accession Number 1Z09.

* Corresponding author. E-mail: Julian.Peterson@UTSouthwestern.edu; tel.: (214) 648-2361; fax: (214) 645-9361.

[§] The University of Texas Southwestern Medical Center at Dallas.

[||] The University of Texas at Dallas.

[1] Abbreviations: EET, epoxyeicosatrienoic acid; AA, arachidonic acid; OH-AA, hydroxyarachidonic acid; PA, palmitic acid; OH-PA, hydroxypalmitic acid; FAD, flavin adenine dinucleotide; FMN, flavin mononucleotide; FNR, ferredoxin-NADP+ reductase; BMP, the individually expressed heme domain of P450BM-3; BMR, the individually expressed reductase domain of P450BM-3; NPG, *N*-palmitoylglycine; NPM, *N*-palmitoyl-L-methionine; NPL, *N*-palmitoyl-L-leucine; NMR, nuclear magnetic resonance; GC-MS, gas chromatography-mass spectrometry; NADPH, nicotinamide adenine dinucleotide phosphate (reduced form); NADP+, nicotinamide adenine dinucleotide phosphate (oxidized form); PEG, polyethylene glycol; MES, 2-(*N*-morpholino)-ethanesulfonic acid; V_{max}, maximal velocity; K_D, dissociation constant.

10.1021/bi701667m CCC: $37.00
Published on Web 11/16/2007

Previously, the three domains of the P450BM-3 fusion protein (heme-binding, BMP (*14*); FAD-binding, FNR-like; and FMN-binding, flavodoxin-like (*15*)) have been expressed separately as well as in various combinations, including the reductase domain BMR (*16*), the individual FAD- and FMN-binding domains, and the FMN-binding domain linked to the heme-binding P450 domain (*17*). In a reconstitution system, the product profile remains the same, although the turnover of the enzymes is significantly decreased (*18*). The structure of substrate-free BMP has been determined by X-ray crystallographic techniques (*19*), and two structures have thus far been published with a substrate bound: one with palmitoleic acid (*20*) and one with *N*-palmitoylglycine (NPG) (*21*). In both cases, the omega end of the fatty acid is located in the heme pocket in similar orientations. The carboxylate groups of both substrates form hydrogen bonds with Tyr51, with that of NPG establishing two additional hydrogen bonds with the backbone amide nitrogen atoms of Gln73 and Ala74 (*21*). Furthermore, favorable electrostatic interactions likely exist between the carboxylate of NPG and the helical dipole of the B′ helix. These additional interactions were proposed to increase the binding affinity of NPG for P450BM-3 and BMP (*21*).

An examination of the crystal structure of NPG bound BMP showed that there is a solvent exposed hydrophobic surface very close to the glycine moiety. We have referred to this surface as the substrate recognition region (*19*) because it is on the surface of the protein in juxtaposition to the substrate access channel. We presumed that hydrophobic fatty acids would initially be bound to this hydrophobic patch and then would enter the substrate access channel. On the basis of this structural information, we hypothesized that if L-amino acid derivatives of palmitic acid were synthesized and used as substrates of BMP, the side chain of the amino acid should interact with this hydrophobic surface. Additional fatty acid derivatives have been synthesized to better understand the factors that are involved in fatty acid binding. We report here new high affinity substrates of P450BM-3 and the crystal structure determination of *N*-palmitoyl-l-methionine (NPM) bound BMP.

EXPERIMENTAL PROCEDURES

General Methods. The heme-binding domain of P450BM-3 and the holoenzyme were purified as previously described (*14*, *15*). The concentrations of either BMP or P450BM-3 were determined by the method of Omura and Sato (*22*). UV−vis spectroscopy was performed on either a Hewlett-Packard model 8452A Diode Array spectrophotometer or a Varian Cary model 100 double beam spectrophotometer.

Synthesis and Characterization of N-Acyl Amino Acids. *N*-Palmitoyl amino acid derivatives were synthesized using the corresponding commercially available *N*-hydroxysuccinimidyl fatty acids and the amino acid by methods previously established for the fatty acylation of amino acids (*23*). The products were recrystallized from ethanol/10 mM HCl. Purity and identities were confirmed by ^{1}H NMR and GC-MS.

Substrate Characterization. For the measurement of oxygen concentration, a solution of 300 μM substrate and 300 μM NADPH in 50 mM potassium phosphate, pH 7.4 was placed in the fiberoptic oxygen sensor apparatus Model 110 from Instech Labs, Inc. (Plymouth Meeting, PA) at 25 °C. The oxygen sensor was calibrated by using the normal reaction mixture with excess NPG as substrate. A standardized aliquot of NADPH was added to the reaction mixture, and the deflection of the oxygen sensor was determined. In those experiments, to determine the rate of oxygen consumption, P450BM-3 was added to the reaction mixture last. The turnover number was calculated from the initial velocity of the reaction. In separate experiments, NADPH consumption was monitored by the change in UV−vis absorption at 340 nm, with concentrations of substrate and NADPH of 100 μM. The turnover number in this instance was calculated using an extinction coefficient of 6220 M^{-1} cm^{-1} for NADPH.

For binding studies, 1.2 mL of a solution of 2.5 μM BMP in 50 mM potassium phosphate, pH 7.4 was titrated with a solution of 1 mM substrate in 50 mM potassium carbonate in a stirred 1.00 cm quartz cuvette. After the addition of each aliquot of substrate, the solution was allowed to equilibrate for 1 min before the UV−vis absorbance spectrum was recorded. Dissociation constants were obtained by fitting the difference between the absorbance at 418 and 392 nm to an equation describing a bimolecular association reaction (*21*).

Substrate Binding to P450BM-3 Mutated at Residue R47. P450BM-3 was mutated to R47Q and R47S using Stratagene's Quik Change II Site Directed Mutagenesis Kit following the manufacturer recommended protocols. The presence of the desired mutations and absence of undesirable mutations was confirmed by DNA sequencing of the entire gene. The proteins were expressed in *Escherichia coli* DH5αF'IQ (Invitrogen) using conditions typical for wild type P450BM-3 (*14*, *15*). Both were expressed at over 50 mg protein/L culture. The enzymes were purified by Ni-NTA chromatography. Titrations with *N*-myristoyl-L-methionine were carried out as performed for titrations of BMP with acyl amino acids.

Complex Formation and Crystallization. For complex formation, BMP (20 μM BMP in 50 mM potassium phosphate, pH 7.4) was titrated with 10 mM NPM in 50 mM potassium carbonate to 10% beyond the equivalence point. The extent of complex formation was established by monitoring the changes in the UV−vis spectrum. This solution was then concentrated in an Amicon centriprep-30 concentrator to a final concentration of 105 μM (12.5 mg/mL). The solution was stored in small aliquots at −80 °C.

Crystals of the BMP−NPM complex were grown using vapor diffusion in the sitting drop format. The precipitant solution was composed of 12% (w/v) PEG-3350, 100 mM $MgCl_2$, 2.5% (v/v) glycerol, 100 mM 2-(N-morpholino)-ethanesulfonic acid (MES), pH 6.5. Equal volumes (2 μL each) of the 4 °C well solution and the 12.5 mg/mL BMP−NPM complex were mixed by pipet, and the wells were sealed. After 24 h equilibration at 4 °C, crystallization was induced by streak seeding from lower quality crystals grown spontaneously at higher PEG-3350 concentrations. Large numbers of crystals typically formed within 24 h. Crystals were transferred to a solution composed of 15% (w/v) PEG-3350, 100 mM $MgCl_2$, 15% (v/v) glycerol, and 100 mM MES, pH 6.5 and incubated 1 h for cryoprotection before being mounted in a nylon loop. Mounted crystals were flash-cooled in liquid propane and stored in liquid nitrogen until used for data collection.

Table 1: Data Collection and Refinement Statistics[a]

Data Collection	
PDB ID code	1ZO9
space group	$P2_1$
a (Å)	59.0
b (Å)	147.8
c (Å)	63.6
β (°)	98.60
wavelength (Å)	1.54178
resolution range (Å)	29.6−1.70 (1.73−1.70)
unique reflections	104145 (2889)
Multiplicity	2.8 (2.4)
data completeness (%)	88.0 (49.1)
R_{merge} (%)[b]	3.0 (26.5)
$I/\sigma(I)$	24.8 (2.9)
Wilson *B* value (Å^2)	**27.6**
Refinement	
resolution range (Å)	29.6−1.70 (1.80−1.70)
no. of reflections R_{work}/R_{free}	100627/5358
atoms (non-H protein/heme/NPM)	7355/1156/52
atoms (non-H MES/glycerol/solvent)	24/84/1072
R_{work} (%)	16.4
R_{free} (%)	19.9
rms deviation bond length (Å)	0.011
rms deviation bond angle (deg)	1.57
σ_A cross-validated coordinate error (Å)	0.13
mean *B* value (Å^2)	26.1
alternate conformations	20
missing residues	A459−A470, B459−B470

[a] Data for the outermost shell are given in parentheses. [b] $R_{merge} = 100\ \Sigma_h\Sigma_i|I_{h,i} - \langle I_h\rangle|/\Sigma_h\Sigma_i I_{h,i}$, where the outer sum (*h*) is over the unique reflections, and the inner sum (*i*) is over the set of independent observations of each unique reflection.

Data Collection. Diffraction data were collected from a single crystal at 110 K, using an R-axis IV imaging plate system (MSC) mounted on a Rigaku RU-200 rotating anode generator (Rigaku) operated at 100 mA and 50 kV. BMP−NPM crystallized with the symmetry of space group $P2_1$ (unit cell constants $a = 59.0$ Å, $b = 147.8$ Å, $c = 63.6$ Å, $\beta = 98.60°$) and contained two molecules per asymmetric unit. All data were processed in the HKL2000 program suite (*24*). Intensities were converted to structure factor amplitudes and placed on an approximate absolute scale by the program TRUNCATE from the CCP4 package (*25*). Data collection and processing statistics are summarized in Table 1.

Crystallographic Refinement. Refinement of the structure of BMP−NPM was carried out in the program package CNS 1.0 (*26*) with a random 5% subset of all data set aside for an R_{free} calculation. Initial model coordinates were obtained by modifying the coordinates of BMP complexed with NPG (PDB code: 1JPZ) (*21*) by removing the coordinates for water molecules and the substrate. Rigid-body refinement of the model coordinates versus data between 20.0 and 2.5 Å was conducted, followed by a cycle of standard positional and group isotropic atomic displacement parameter refinement. Inspection of electron-density maps in the program O (*27*) allowed a model for the substrate to be added. Subsequent cycles of standard positional and individual isotropic atomic displacement parameter refinement coupled with cycles of model rebuilding, modeling of alternate conformations, and addition of solvent molecules were carried out against all data from 29.6 to 1.70 Å. Complete refinement statistics for the structure are listed in Table 1.

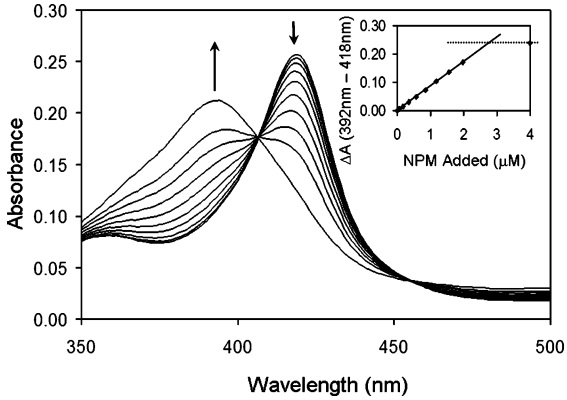

FIGURE 1: Titration of BMP with NPM. BMP (2.5 μM) in potassium phosphate buffer (50 mM, pH 7.4) was titrated with NPM. The arrows in the figure indicate the direction of change of absorbance upon each addition. The inset in the figure is the calculated difference in absorbance for the wavelength pair 392 and 418 nm plotted vs the concentration of NPM added to the reaction mixture. After the addition of an excess of NPM, the absorbance does not change (only 4 μM is shown, but the absorbance difference was constant through more than 10 μM substrate).

RESULTS

Synthesis and Binding of Fatty Acid Derivatives to BMP. The addition of fatty acids to solutions of P450BM-3 or its heme domain (BMP) has been shown to result in a shift of the absorbance maximum of the Soret band from 418 to 392 nm, indicative of the conversion of the heme iron from low- to high-spin. The extent of this conversion was found to correlate with the chain length of the fatty acid, with the maximal extent of conversion observed for saturated fatty acids of chain length C14 or C16 (*1*). Polyunsaturated fatty acids such as arachidonic or linolenic acid also cause the shift from the low- to high-spin state (*11*). Recently, we demonstrated that the preparation of the fatty acid amide derivative of glycine significantly enhances the binding of palmitic acid to BMP without changing the regioselectivity of oxidation of the fatty acid moiety (*21*). X-ray crystal structure analysis of these substrates bound to BMP revealed the formation of two additional hydrogen bonds to the amino acid backbone amide nitrogen atoms in the B′ helix (*21*) as compared to the palmitoleic acid bound BMP structure (*20*). Under the conditions of those experiments, the equilibrium dissociation constant for palmitic acid was 1.3 μM, while that of NPG was 0.3 μM.

In an effort to further understand the factors that influence the binding affinities of various molecules to P450s, a series of amino acid derivatives of palmitic acid was synthesized with the expectation that they might bind well to P450BM-3. Their interaction with BMP and oxidation by P450BM-3 was examined. As can be seen in an example titration of BMP with NPM shown in Figure 1, the addition of the fatty acid derivative results in the conversion of the low- to the high-spin form of the protein with isosbestic points at 406 and 457 nm and (not shown) isosbestic points at 531, 586, and 682 nm. Shown in the inset to Figure 1 is a plot of the increase in absorbance at 392 nm minus the decrease in absorbance at 418 nm as a function of the concentration of NPM. The absorbance difference increases linearly as a function of the concentration of analogue added prior to the equivalence point (determined as the point at which the linear

Table 2: Fatty Acid Binding by BMP[a]

substrate	K_D (μM)
palmitic acid	1.3 ± 0.2
N-palmitoylglycine	0.32 ± 0.01
N-palmitoylglycylglycine	6.65 ± 0.65
N-palmitoyl-L-methionine	<0.008
N-palmitoyl-L-glutamine	0.30 ± 0.01
N-palmitoyl-L-glutamic acid	3.7 ± 0.1
N-palmitoyl-L-leucine	<0.008
N-palmitoyl-L-phenylalanine	0.41 ± 0.08
lauric acid	N.D.
N-lauroylglycine	304 ± 30

[a] Dissociation constants were determined using 2.5 μM BMP in 50 mM potassium phosphate buffer, pH 7.4 titrated with a solution of 1 mM substrate in 50 mM potassium carbonate in a stirred 1.00 cm quartz cuvette. The data for the absorbance at 418 nm minus the absorbance at 392 nm were corrected for dilution and fitted to an equation for a bimolecular association reaction to obtain the dissociation constant.

portion intersects with a line representing the constant absorbance difference observed upon the addition of excess fatty acid analogues). As expected, the equivalence point is observed at a stoichiometry of one molecule of analogue bound per molecule of BMP in solution. The fatty acid analogue bound too tightly to allow reliable estimation of the dissociation constant from this experiment.

We performed a similar titration of 0.25 μM BMP with *N*-palmitoyl-L-leucine (NPL). For the final point on the linear portion of this titration (0.2 μM NPL added), we estimated that no more than 10% of the fatty acid analogue was free, while the remaining material was bound to BMP as measured by the absorbance change. Inserting these values into the equation for a dissociation reaction, the value of approximately 8 nM is obtained. We believe that this is the maximum value for this dissociation constant; however, the equilibrium dissociation constant could be significantly smaller than this value if less than 10% of the fatty acid analogue was free in solution as postulated previously. Both NPM and NPL were determined to have dissociation constants no larger than 8 nM.

To explore the effect of other amino acid side chains on fatty acid binding, we synthesized the fatty acid derivatives listed in Table 2. As indicated previously, the presence of the hydrophobic side chain of NPM substantially decreased the dissociation constant. NPL was also bound by BMP extremely well, with a dissociation constant of less than the value that we could measure by our spectrophotometric-binding assay. In contrast, the binding of the glycylglycine analogue, which should be significantly more polar than the parent glycine analogue, was substantially reduced when compared to either NPG or even free palmitic acid. Increasing the polarity of the amino acid side chain increased the dissociation constant for the analogues. It was somewhat surprising that *N*-palmitoyl-L-phenylalanine did not bind to BMP more tightly than NPG, indicating that the size or shape of the hydrophobic side chain of the amino acid residue limits the binding to BMP.

Lauric acid is commonly used as a model substrate for P450BM-3, even though it shows little conversion of the heme iron from low- to high-spin, making the binding constant difficult to determine by UV−vis titration. As can be seen in Table 2, the glycine derivative of lauric acid shows enhanced binding as compared to the free acid, and the binding constant could be determined.

Table 3: *N*-Myristoyl-L-methionine Binding by P450BM-3 and Its Mutants[a]

enzyme	K_D (μM)
BMP	1.0 ± 0.3
P450BM-3	0.8 ± 0.2
P450BM-3(R47Q)	2.2 ± 0.2
P450BM-3(R47S)	1.9 ± 0.1

[a] Dissociation constants were determined using 2.5 μM BMP, P450BM-3, or a mutant of P450BM-3 in 50 mM potassium phosphate buffer, pH 7.4 titrated with a solution of 1 mM substrate in 50 mM potassium carbonate in a stirred 1.00 cm quartz cuvette. The data for the absorbance at 418 nm minus the absorbance at 392 nm were fitted to an equation for the bimolecular association reaction to obtain the dissociation constant.

Substrate Binding to P450BM-3 Mutants Lacking a Positive Charge at R47. An arginine at position 47 of the amino acid sequence of P450BM-3 has been shown to provide important interactions with the anionic fatty acid substrates but appears to have much less interaction with NPG (*21*). We assume that the R47 side chain is positively charged. To further examine the role of the R47 charge in controlling substrate binding, we carried out a comparative study of substrate binding to wild type P450BM-3 and two charge neutralized mutants, R47Q and R47S. Because the tight binding of NPM would prevent the comparison of very similar K_D values, we instead used *N*-myristoyl-L-methionine, which binds more weakly due to its reduced hydrophobic surface area. The results appear in Table 3. On the basis of the trend of K_D values for acyl glycines with varying chain lengths, the binding constant for *N*-myristoyl-L-methionine would be expected to be approximately 30-fold higher than that for the palmitoyl analogue (since the addition of 4 methylene groups to NPG relative to *N*-lauroylglycine results in an ~1000-fold increased affinity, two methylene groups would be predicted to increase the affinity by the square root of 1000). This is indeed the case, with the measured K_D value of 1.0 μM for BMP and 0.8 μM for P450BM-3 agreeing very well with the 0.9 μM K_D value predicted by this method. The good agreement results from a fairly constant increase in free energy of substrate binding as the acyl chain length (and hydrophobic surface area) is increased.

For both of the charge neutralized mutants, binding of the anionic acyl methionine was weaker, supporting an interaction between the positive charge of R47 and the substrate carboxylate even in acyl amino acids, where the carboxylate charge also interacts with the helix dipole of the B′ helix. The magnitude of the change was relatively small, with only a 2−3-fold decrease in affinity when the positive charge was removed by mutation. This result is in good agreement with previous work described in the literature on the binding of substrates to R47 mutants (see Discussion).

Rate of Oxidation of NADPH Is Dependent on Fatty Acyl Amide Derivatives. Our previous studies of the oxidation of NPG by BMP showed that the rate was somewhat faster than that of the parent compound palmitic acid. To continue our analysis, we also measured the rates of oxidation of the other derivatives of palmitic acid. The rate of oxidation of NADPH is a good measure of the production of hydroxylated products, as we have previously established that NADPH oxidation is highly coupled to substrate hydroxylation for NPG, as with most substrates of P450BM-3. As can be seen in Table 4, the rate of oxidation of NADPH, as measured

Table 4: Rate of Oxidation of Fatty Acid Derivatives by P450BM-3

substrate	k_{cat} (min^{-1})
palmitic acid	1480 ± 35
N-palmitoylglycine	1880 ± 30
N-palmitoyl-L-methionine	1690 ± 75
N-palmitoyl-L-glutamine	610 ± 25
N-palmitoyl-L-glutamic acid	485 ± 15
N-palmitoyl-L-leucine	1160 ± 20

by the change in absorbance at 340 nm, was maximal with NPG as substrate and almost as high with NPM. As expected, the rate of oxidation of NADPH was significantly lower for the more polar fatty acid analogues than that of the nonpolar molecules. It should be noted that the ratio of the rate of oxidation of NPG to palmitic acid was 1.3:1, whereas in one of our previously published experiments, we observed a ratio of 1.4:1 (*21*). We believe that this difference is within the normal variability for measurements of the rate of P450BM-3 reactions by different researchers using different enzyme preparations. Additionally, as will be discussed in a subsequent manuscript, the value determined for the turnover number of P450BM-3 with any given substrate is extremely sensitive to differences in conditions due to partial protein dimerization; thus, it is difficult to make absolute comparisons of these values.

Crystal Structure of NPM Bound BMP. As described previously, NPM binds very tightly to BMP and thus makes a very good candidate for an X-ray structural analysis. A slight molar excess of the substrate over BMP was added to a dilute solution of the protein, and the conversion from low- to high-spin was observed by absorbance spectrophotometry. The solution was concentrated, and high quality crystals were grown as described in the Experimental Procedures. The crystals had a unit cell that was isomorphous to the BMP-NPG structure (*21*) and diffracted X-rays generated by an in-house generator to a Bragg spacing (d_{min}) of about 1.6 Å. The structure was refined using diffraction data to a d_{min} value of 1.70 Å. The asymmetric unit contained two copies of the complex and included two hemes, two NPM ligands, two molecules of MES buffer, 14 glycerol molecules, 1072 molecules of solvent, and all protein residues except for the C-terminus (residues 459−470) in each monomer. Figure 2 shows an overview of molecule A (as discussed next, molecule B is essentially identical).

The refined structure of BMP−NPM is very similar to that of the previously determined BMP−NPG (*21*). The two monomers in the asymmetric unit differ from each other by a larger amount than do the lattice-equivalent monomers for the different substrate complexes. The differences are primarily due to differences in lattice contacts for the two monomers in this crystal form. The two monomers within the asymmetric unit of BMP−NPM superimpose with an rms deviation of 0.24 Å for 451 common Cα atoms, very similar to the rms deviation of 0.28 Å for the two monomers of the BMP−NPG complex. The superposition of the lattice-equivalent monomers (A or B, as defined in the PDB file) of BMP−NPM and BMP−NPG yields rms deviations of 0.10 Å for both molecules (451 common Cα atoms.) As in the previous structure, the acyl chain of the fatty acyl amino acid extends into the hydrophobic active site of the enzyme in the same manner as previously observed for fatty acid substrates (*20*). The substrate amide carbonyl is in position

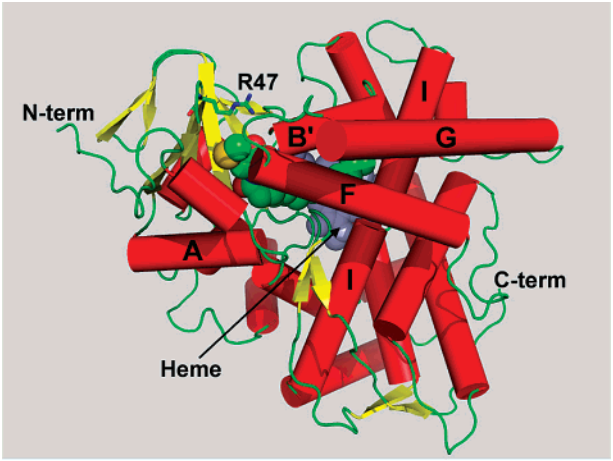

FIGURE 2: Backbone structure of NPM complexed to BMP. Helices are red cylinders, strands are yellow, and loops are green. The bound substrate appears as space-filling spheres colored by atom type with green carbon atoms. The heme (partially obscured) is shown as space-filling spheres in light blue. Residue R47 (top, stick representation colored by atom type) protrudes to the surface of the enzyme, unlike previous structures of substrate bound or free BMP.

to accept a hydrogen bond from Y51 as observed for the carboxylate of palmitoleic acid and the amide carbonyl of NPG. The carboxylate of the substrate interacts with the uncapped B′ helix as observed for NPG, likely contributing to the high affinity of the enzyme for these substrates. Thus, the major interactions leading to the high affinity of NPG for P450BM-3 appear to be conserved in NPM.

The major differences between the structures of the two substrate−enzyme complexes occur at the binding site for the NPM amino acid side chain. This hydrophobic side chain extends toward the surface of the protein in the region of residue R47 (Figures 2 and 3). To accommodate the side chain of the substrate, an ordered water molecule in the NPG bound structure (HOH818 in molecule A, PDB code 1JPZ) has been displaced, and the side chain of R47 has rotated away from the substrate. This side chain, which has previously been shown to provide important interactions with the anionic substrates of P450BM-3, now extends into solution at the surface of the protein. The result of the new orientation of R47 and of displacement of the water molecule is the formation of a hydrophobic pocket in which the substrate's hydrophobic amino acid side chain resides. These features provide a structural basis for the increase in affinity for small hydrophobic side chains and for the observation that large rigid side chains do not bind as well (due to an improper fit into this pocket).

DISCUSSION

Newly discovered interactions accessible in the P450BM-3 active site have allowed the design of novel, extremely potent substrates for this enzyme. One such interaction is the previously discovered interaction of the carboxylates of acyl amino acids with the uncapped N-terminal backbone amides of the B′ helix (*21*). Exploitation of a hydrophobic cleft available to amino acid side chains results in even stronger interactions with the enzyme.

Desolvation of the amino acid side chain appears to be responsible for most of the differences in binding affinity

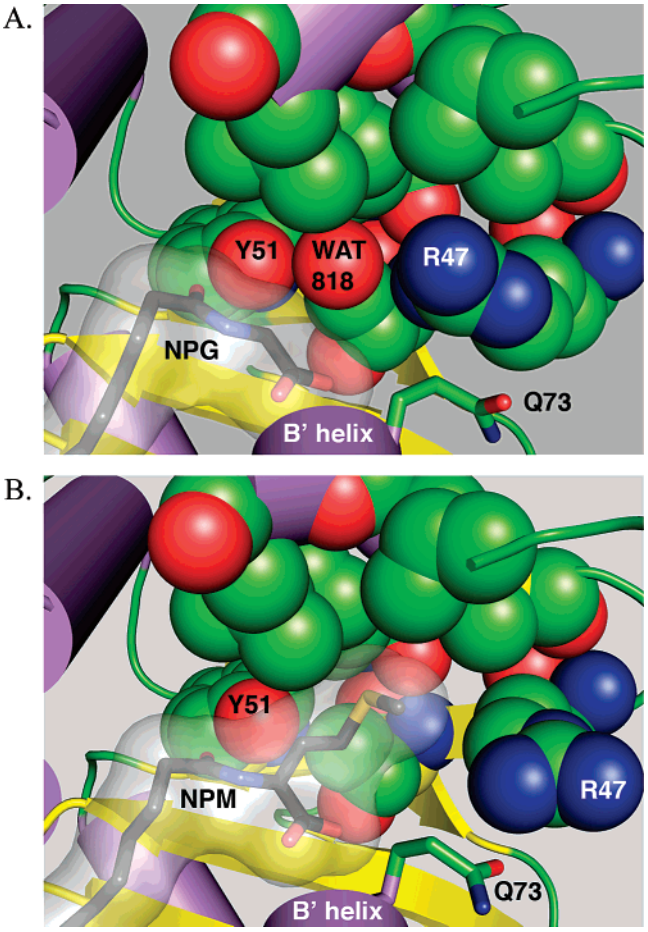

FIGURE 3: Comparison of *NPG* and NPM binding to BMP. Residues and water in the substrate recognition pocket of BMP are shown as space-filling spheres, Q73 and the substrate are represented as stick models, and a transparent surface is drawn around the substrate. Helices are red cylinders, strands are yellow, and loops are green. Protein carbon atoms are green and substrate carbon atoms are white, oxygens are red, nitrogens are blue, and sulfurs are yellow. (A) NPG bound BMP and (B) NPM bound BMP.

within the series of compounds because binding free energies (derived from the dissociation constants) for acyl amino acid binding to P450BM-3 and free energies of side chain desolvation of *N*-acetyl amino acids (*28*, *29*) derived from water−octanol partitioning show good correlation with the exception of the phenylalanine derivative. In general, the difference in the P450BM-3-binding energy for two compounds is roughly twice the difference in the side chain desolvation energy. This relationship is expected if an area of the hydrophobic enzyme active site is roughly equal to the surface area of the bound amino acid side chain and also desolvates upon binding (*30*). This result implies that the side chain-binding pocket is either preformed or requires little energy to form. The small rearrangements in the protein in response to the binding of the methionine side chain are consistent with a very low energy rearrangement. The desolvation in this case appears to consist primarily of the expulsion of a single water molecule.

Taking advantage of the structural features of the substrate-binding pocket has allowed us to create substrates that bind very tightly to the enzyme but still turnover at near the maximal reported rate. When comparing V_{max}/K_D, *N*-palmitoyl-L-leucine and NPM are the best substrates ever reported for this enzyme. In fact, they are probably the best substrates ever reported for any cytochrome P450. Typical P450 substrates generally have dissociation constants in the 0.1−100 μM range, although some examples exist of substrates with dissociation constants in the low nanomolar range (*31*, *32*). P450BM-3 has a much higher turnover number than the typical P450, however, and these appear to be the only P450 monooxygenation substrates reported with K_D values below 100 nM combined with turnover numbers in excess of 1000 μmol/min/μmol.

The affinity of these substrates approaches empirical limits for ligands of their size for any protein. An analysis of the affinity of ligands for proteins as a function of ligand size (number of non-carbon atoms) revealed that the maximum affinity of a ligand with 26 non-hydrogen atoms (the size of NPM and *N*-palmitoyl-L-leucine) observed in nature (for ligands that do not bind metals) is approximately 0.5−1 nM (*33*). The ligands with the highest affinity bind to active sites that do not require significant reorganization, so no binding energy is wasted to induce active site rearrangements. The binding energy of fatty acyl substrates of P450BM-3 must have a component accounting for structural rearrangements of the protein. One specific example is an unfavorable rotation of the phenyl ring of F87 coupled to substrate binding (*20*). The energy investment required, which was estimated by comparison of dissociation constants for a given substrate for wild type and F87A or F87V mutant P450BM-3, ranges from 0.5−5 kJ/mol for various substrates described in the literature (*34*). Without that required investment of energy, substrates could bind more tightly. The dissociation constants for our substrates if they were not required to make this investment can be estimated by separating the energies of substrate binding and protein rearrangement. The affinity of substrate for enzyme in the absence of the investment can be determined from the relationships $\Delta G_{measured} = \Delta G_{binding} + \Delta G_{investment} = -RT \ln(K_{D-measured})$ and $K_{D-binding} = \exp(-\Delta G_{binding})/RT$. Accordingly, an affinity of 8 nM for NPM binding to wild type P450BM-3 would be predicted to be 1−7 nM in the absence of the F87 rearrangement. Larger rearrangements are the movement of the I helix and the coupled movement of the F− and G helices upon substrate binding. Little is known about the energetics of this rearrangement, which is responsible for the spin state change that occurs upon substrate binding (*20*, *21*). If this rearrangement costs even a few kilojoules per mole, the affinity of our substrates must be near the limit practically obtainable for P450BM-3 ligands of this size (that do not interact with the heme iron).

Our earlier report of the crystal structure of the heme domain of P450BM-3 complexed to a new, more potent (and soluble) substrate NPG had a great impact on the feasibility of studies using low affinity fatty acid substrates. Because of the high concentrations required, low aqueous solubility, and inherent amphipathic properties of the fatty acids, many studies suffer from nonspecific aggregation of the substrate and nonspecific binding of excess substrate to the enzyme. The increased affinity and solubility of NPG can circumvent many of these problems. The substrates reported here, which include compounds with at least 1 order of magnitude higher affinity for the enzyme than even NPG, now provide a range of compounds with similar properties to promote studies of P450 structure and function.

This newly expanded class of high affinity, soluble substrates of P450BM-3 retains nearly all of the interactions with P450BM-3 that comparable fatty acids exploit, such as the hydrogen bond to Y51 and the hydrophobic interactions that are the dominating force driving binding. Our data demonstrate that some interaction between the carboxylate negative charge and the positive charge of R47 is retained, even though the carboxylate now also interacts with the B′ helix dipole.

The magnitude of the R47−substrate interaction, although somewhat weaker, is consistent with previous data on R47 mutants (*35*). For example, the binding of palmitoleic acid to the R47A mutant has been studied (*35*), revealing a K_D value of 7 ± 1 μM for palmitoleic acid. This affinity is about 5 times higher than that for the wild type enzyme (34 ± 5 μM). Those binding constants correspond to a loss of 4.1 ± 0.8 kJ/mol binding energy upon R47 charge neutralization. Our two charge neutralized mutants demonstrated an average loss of 2.3 kJ/mol of binding free energy. The minimum distance between R47 and substrate carboxylate in our NPM structure was nearly twice that of palmitoleic acid bound to BMP. For palmitoleic acid bound to BMP (1FAG), the distance ranges from 3.5−4.8 Å, for NPG (1JPG) 4.5−4.8 Å, and 6.5−7.5 Å in the NPM structure reported here. On the basis of a $1/r$ dependence of electrostatic free energy, the 4.1 kJ/mol free energy of binding attributable to the electrostatic contribution of R47 at an average distance of 4.2 Å for palmitoleic acid would be predicted to weaken to 2.4 kJ/mol at a distance of 7.0 Å, the average for our NPM bound structure. This prediction agrees very well with our observed loss of 2.3 kJ/mol binding energy for *N*-myristoyl-L-methionine when the charge at R47 is neutralized, suggesting that the altered conformation for this residue observed in our low temperature crystal structure is also relevant in solution at room temperature.

The tight binding of the compounds may also provide clues about the role of P450BM-3 in vivo. There are many emerging examples of acyl amino acids that play a signaling role in bacterial symbiosis and pathogenesis in nature. Volicitin (17-hydroxylinolenoyl-L-glutamine), for example, is synthesized in a complex interaction of plant, army worm, and army worm gut bacteria. The plant changes its odor in response to volicitin, which serves as a chemical signal that an army worm is preying on the plant, to attract wasps that will kill the attacking worm (*36*−*40*). Interestingly, the biosynthesis of volicitin involves the ω-1 hydroxylation of linolenoyl-L-glutamine (or of linolenic acid prior to conjugation to glutamine). Acyl homoserine lactones have received considerable attention in the past few years for their role in quorum sensing, the process by which bacteria sense their own concentration for determining the appropriate time to involve themselves in symbioses or when to express pathogenic genes (for recent reviews, see refs *41* and *42*).

REFERENCES

1. Narhi, L. O., and Fulco, A. J. (1986) Characterization of a catalytically self-sufficient 119 000 Da cytochrome P450 monooxygenase induced by barbiturates in *Bacillus megaterium*, *J. Biol. Chem. 261*, 7160−7169.
2. Narhi, L. O., Kim, B. H., Stevenson, P. M., and Fulco, A. J. (1983) Partial characterization of a barbiturate-induced cytochrome P450-dependent fatty acid monooxygenase from *Bacillus megaterium*, *Biochem. Biophys. Res. Commun. 116*, 851−858.
3. Wen, L. P., and Fulco, A. J. (1987) Cloning of the gene encoding a catalytically self-sufficient cytochrome P450 fatty acid monooxygenase induced by barbiturates in *Bacillus megaterium* and its functional expression and regulation in heterologous (*Escherichia coli*) and homologous (*Bacillus megaterium*) hosts, *J. Biol. Chem. 262*, 6676−6682.
4. Narhi, L. O., and Fulco, A. J. (1987) Identification and characterization of two functional domains in cytochrome P450BM-3, a catalytically self-sufficient monooxygenase induced by barbiturates in *Bacillus megaterium*, *J. Biol. Chem. 262*, 6683−6690.
5. Miura, Y., and Fulco, A. J. (1975) Omega-1, Omega-2, and Omega-3 hydroxylation of long-chain fatty acids, amides, and alcohols by a soluble enzyme system from *Bacillus megaterium*, *Biochim. Biophys Acta 388*, 305−317.
6. Narhi, L. O., and Fulco, A. J. (1982) Phenobarbital induction of a soluble cytochrome P450-dependent fatty acid monooxygenase in *Bacillus megaterium*, *J. Biol. Chem. 257*, 2147−2150.
7. Ruettinger, R. T., Kim, B. H., and Fulco, A. J. (1984) Acylureas: A new class of barbiturate-like bacterial cytochrome P450 inducers, *Biochim. Biophys. Acta 801*, 372−380.
8. English, N., Hughes, V., and Wolf, C. R. (1996) Induction of cytochrome P450BM-3 (CYP 102) by non-steroidal anti-inflammatory drugs in *Bacillus megaterium*, *Biochem. J. 316*, 279−283.
9. English, N., Palmer, C. N., Alworth, W. L., Kang, L., Hughes, V., and Wolf, C. R. (1997) Fatty acid signals in *Bacillus megaterium* are attenuated by cytochrome P450-mediated hydroxylation, *Biochem. J. 327*, 363−368.
10. Palmer, C. N., Axen, E., Hughes, V., and Wolf, C. R. (1998) The repressor protein, Bm3R1, mediates an adaptive response to toxic fatty acids in *Bacillus megaterium*, *J. Biol. Chem. 273*, 18109−18116.
11. Capdevila, J. H., Wei, S., Helvig, C., Falck, J. R., Belosludtsev, Y., Truan, G., Graham-Lorence, S. E., and Peterson, J. A. (1996) The highly stereoselective oxidation of polyunsaturated fatty acids by cytochrome P450BM-3, *J. Biol. Chem. 271*, 22663−22671.
12. Truan, G., Komandla, M. R., Falck, J. R., and Peterson, J. A. (1999) P450BM-3: Absolute configuration of the primary metabolites of palmitic acid, *Arch. Biochem. Biophys. 366*, 192−198.
13. Graham, S. E., and Peterson, J. A. (2002) Sequence alignments, variabilities, and vagaries, *Methods Enzymol. 357*, 15−28.
14. Boddupalli, S. S., Hasemann, C. A., Ravichandran, K. G., Lu, J. Y., Goldsmith, E. J., Deisenhofer, J., and Peterson, J. A. (1992) Crystallization and preliminary X-ray diffraction analysis of P450terp and the hemoprotein domain of P450BM-3, enzymes belonging to two distinct classes of the cytochrome P450 superfamily, *Proc. Natl. Acad. Sci. U.S.A. 89*, 5567−5571.
15. Sevrioukova, I., Truan, G., and Peterson, J. A. (1996) The flavoprotein domain of P450BM-3: Expression, purification, and properties of the flavin adenine dinucleotide- and flavin mononucleotide-binding subdomains, *Biochemistry 35*, 7528−7535.
16. Oster, T., Boddupalli, S. S., and Peterson, J. A. (1991) Expression, purification, and properties of the flavoprotein domain of cytochrome P450BM-3. Evidence for the importance of the amino-terminal region for FMN binding, *J. Biol. Chem. 266*, 22718−22725.
17. Sevrioukova, I. F., Li, H., Zhang, H., Peterson, J. A., and Poulos, T. L. (1999) Structure of a cytochrome P450-redox partner electron-transfer complex, *Proc. Natl. Acad. Sci. U.S.A. 96*, 1863−1868.
18. Sevrioukova, I., Truan, G., and Peterson, J. A. (1997) Reconstitution of the fatty acid hydroxylase activity of cytochrome P450BM-3 utilizing its functional domains, *Arch. Biochem. Biophys. 340*, 231−238.
19. Ravichandran, K. G., Boddupalli, S. S., Hasemann, C. A., Peterson, J. A., and Deisenhofer, J. (1993) Crystal structure of hemoprotein domain of P450BM-3, a prototype for microsomal P450's, *Science (Washington, DC, U.S.) 261*, 731−736.
20. Li, H., and Poulos, T. L. (1997) The structure of the cytochrome p450BM-3 haem domain complexed with the fatty acid substrate, palmitoleic acid, *Nat. Struct. Biol. 4*, 140−146.
21. Haines, D. C., Tomchick, D. R., Machius, M., and Peterson, J. A. (2001) Pivotal role of water in the mechanism of P450BM-3, *Biochemistry 40*, 13456−13465.
22. Omura, T., and Sato, R. (1964) The carbon monoxide-binding pigment of liver microsomes: I. Evidence for its hemoprotein nature, *J. Biol. Chem. 239*, 2370−2378.
23. Lapidot, Y., Rappoport, S., and Wolman, Y. (1967) Use of esters of *N*-hydroxysuccinimide in the synthesis of *N*-acylamino acids, *J. Lipid Res. 8*, 142−145.

24. Otwinowski, Z., and Minor, W. (1997) Processing of X-ray diffraction data collected in oscillation mode, *Methods Enzymol. 276*, 307−326.
25. French, S., and Wilson, K. (1978) On the treatment of negative intensity observations, *Acta Crystallogr., Sect. A: Found. Crystallogr. 34*, 517−525.
26. Brunger, A. T., Adams, P. D., Clore, G. M., DeLano, W. L., Gros, P., Grosse-Kunstleve, R. W., Jiang, J. S., Kuszewski, J., Nilges, M., Pannu, N. S., Read, R. J., Rice, L. M., Simonson, T., and Warren, G. L. (1998) Crystallography and NMR system: A new software suite for macromolecular structure determination, *Acta Crystallogr., Sect. D: Biol. Crystallogr. 54*, 905−921.
27. Jones, T. A., Zou, J. Y., Cowan, S. W., and Kjeldgaard. (1991) Improved methods for building protein models in electron density maps and the location of errors in these models, *Acta Crystallogr., Sect. A: Found. Crystallogr. 47*, 110−119.
28. Creighton, T. E., and Chothia, C. (1989) Protein structure. Selecting buried residues [news], *Nature (London, U.K.) 339*, 14−15.
29. Fauchere, J. L. (1982) A quantitative structure−activity relationship study of the inhibitory action of a series of enkephalin-like peptides in the guinea pig ileum and mouse vas deferens bioassays, *J. Med. Chem. 25*, 1428−1431.
30. Fersht, A. R. (1999) *Structure and Mechanism in Protein Science*, W. H. Freeman and Co., New York.
31. Turner, C. R., Marcus, C. B., and Jefcoate, C. R. (1985) Selectivity in the binding of hydroxylated benzo[*a*]pyrene derivatives to purified cytochrome P450c, *Biochemistry 24*, 5124−5130.
32. Locuson, C. W., II, Rock, D. A., and Jones, J. P. (2004) Quantitative binding models for CYP2C9 based on benzbromarone analogues, *Biochemistry 43*, 6948−6958.
33. Kuntz, I. D., Chen, K., Sharp, K. A., and Kollman, P. A. (1999) The maximal affinity of ligands, *Proc. Natl. Acad. Sci. U.S.A. 96*, 9997−10002.
34. Haines, D. C. (2006) A role for the strained phenylalanine ring rotation induced by substrate binding to cytochrome CYP102A1, *Protein Peptide Lett. 13*, 977−980.
35. Cowart, L. A., Falck, J. R., and Capdevila, J. H. (2001) Structural determinants of active site binding affinity and metabolism by cytochrome P450 BM-3, *Arch. Biochem. Biophys 387*, 117−124.
36. Frey, M., Stettner, C., Pare, P. W., Schmelz, E. A., Tumlinson, J. H., and Gierl, A. (2000) An herbivore elicitor activates the gene for indole emission in maize, *Proc. Natl. Acad. Sci. U.S.A. 97*, 14801−14806.
37. Schmelz, E. A., Alborn, H. T., and Tumlinson, J. H. (2001) The influence of intact-plant and excised-leaf bioassay designs on volicitin- and jasmonic acid-induced sesquiterpene volatile release in *Zea mays*, *Planta 214*, 171−179.
38. Itoh, S., Kuwahara, S., Hasegawa, M., and Kodama, O. (2002) Synthesis of the (17R)- and (17S)-isomers of volicitin, an elicitor of plant volatiles contained in the oral secretion of the beet armyworm, *Biosci. Biotechnol. Biochem. 66*, 1591−1596.
39. Lait, C. G., Alborn, H. T., Teal, P. E., and Tumlinson, J. H., III. (2003) Rapid biosynthesis of *N*-linolenoyl-L-glutamine, an elicitor of plant volatiles, by membrane-associated enzyme(s) in *Manduca sexta*, *Proc. Natl. Acad. Sci. U.S.A. 100*, 7027−7032.
40. Yoshinaga, N., Sawada, Y., Nishida, R., Kuwahara, Y., and Mori, N. (2003) Specific incorporation of L-glutamine into volicitin in the regurgitant of *Spodoptera litura*, *Biosci. Biotechnol. Biochem. 67*, 2655−2657.
41. Federle, M. J., and Bassler, B. L. (2003) Interspecies communication in bacteria, *J. Clin. Invest. 112*, 1291−1299.
42. Dong, Y. H., and Zhang, L. H. (2005) Quorum sensing and quorum-quenching enzymes, *J. Microbiol. 43*, 101−109.

BI701667M